ELSEVIER

Updating robust reliability using structural test data

C. Papadimitriou[a,*], J.L. Beck[b], L.S. Katafygiotis[c]

[a]*Department of Mechanical and Industrial Engineering, University of Thessaly, Pedion Areos, 38334 Volos, Greece*
[b]*Division of Engineering and Applied Science 104-44, California Institute of Technology, Pasadena, CA 91125, USA*
[c]*Department of Civil Engineering, The Hong Kong University of Science and Technology, Clear Water Bay, Kowloon, Hong Kong, People's Republic of China*

Abstract

The concept of robust reliability is defined to take into account uncertainties from structural modeling in addition to the uncertain excitation that a structure will experience during its lifetime. A Bayesian probabilistic methodology for system identification is integrated with probabilistic structural analysis tools for the purpose of updating the assessment of the robust reliability based on dynamic test data. Methods for updating the structural reliability for both identifiable and unidentifiable models are presented. Application of the methodology to a simple beam model of a single-span bridge with soil-structure interaction at the abutments, including a case with a tuned-mass damper attached to the deck, shows that the robust reliabilities computed before and after updating with "measured" dynamic data can differ significantly. © 2001 Elsevier Science Ltd. All rights reserved.

Keywords: System identification; Bayes theorem; Structural reliability; Condition assessment; Model updating; Structural control

1. Introduction

The assessment of the reliability of a structure is not only important during its design but also during its operation. During the design stage, all uncertain factors affecting the assessment of structural safety should be taken into account. Therefore, in addition to the uncertain excitation the structure will experience during its lifetime, the effects of uncertainties arising from modeling errors and assumptions should be included. These modeling uncertainties are usually quantified based on engineering judgment and experience. Using a probabilistic description of these uncertainties, probabilistic structural analysis tools are available for computing estimates of the structural reliability (e.g. Refs. [1–5]).

During operation, the condition, and as a result the reliability, of the structure may deteriorate from fatigue or corrosion, or from damage induced in structural members or joints by a severe loading event such as strong wind loads or earthquakes. Another example of condition change during operation, which is not necessarily related to structural damage, is the detuning of tuned-mass dampers (TMD) installed in a structure to control its vibrational response. This also may lead to significant reduction of the structural

reliability. Therefore, a methodology is needed to re-assess the reliability of the structure after it has been built by monitoring its dynamic response [6,7]. The updated reliability may be used to identify potentially unsafe structures, to schedule inspection intervals [8], repairs or maintenance, or to design retrofitting or control strategies for structures which are thought to be vulnerable to possible future severe loads.

The objective of this study is to present a general framework for a robust measure of structural safety and reliability and a methodology for updating it using dynamic test data. The concept of robustness is used here in a sense similar to that in robust control to mean that modeling uncertainties are taken explicitly into account so that the calculated reliability is not sensitive to these uncertainties [9–14]. More generally, one can define robust analysis to mean the analysis of the response of a system taking modeling uncertainties into account. The framework presented here for the special case of robust reliability applies also to robust analysis.

In this work, robust reliability is defined using the theorem of total probability to be the integral over a specified set of possible models of the conditional reliability for a given model weighted by the probability of that model. To update the robust reliability using measured response data, a Bayesian probabilistic framework for system identification [15–17] is integrated with probabilistic structural dynamics tools. This system identification methodology provides

* Corresponding author. Tel.: +30-421-74-287; fax: +30-421-74-009.
  E-mail address: costasp@mie.uth.gr (C. Papadimitriou).

more accurate representations of the uncertainties associated with the structural modeling because it is based on both measured data and prior engineering information. Using the updated distribution of the system model parameters, a methodology is presented for computing the reliability of structures subjected to uncertain future environmental loads, such as earthquake and wind loads. The methodology is general and can be applied to both linear and non-linear models. It complements a Bayesian probabilistic approach to structural health monitoring which examines the probability of structural damage in prescribed substructures [18–23].

2. Model updating during monitoring

Model updating is used herein to identify and quantify changes in the condition of the structure. These changes along with their corresponding uncertainties are needed for evaluating structural integrity and updating structural reliability. Reviews and textbooks on available model updating techniques based on measured dynamic data can be found in the literature although probability-based approaches are rarely mentioned (e.g. Refs. [24–27]). This section gives a brief summary of a probabilistic system identification methodology [16,17,28,29] which is well-suited for quantifying the modeling uncertainties needed in updating the robust structural reliability. The probabilistic system identification methodology [17] allows for the explicit treatment of the uncertainties arising from both measurement noise and modeling errors by providing a probabilistic description of not only the structural models but also the prediction error for each structural model from a prescribed class of models. It also allows for the explicit treatment of the ill-conditioning and non-uniqueness arising in the model updating inverse problem. Applications of the probabilistic system identification methodology, including illustrative examples, in model updating, damage detection, and optimal sensor location can be found in other Refs. [18–21].

The model updating is handled by embedding a class of structural models $\mathcal{M}$, parameterized by the parameter vector $\boldsymbol{\theta} \in \mathcal{R}^m$, within a class of probabilistic models which account for model prediction error. The vector $\boldsymbol{\theta}$ contains the free parameters which need to be assigned values in order to choose a particular model, designated by $\mathcal{M}(\boldsymbol{\theta})$, in $\mathcal{M}$. Let $\mathbf{q}(n; \boldsymbol{\theta})$ be the model response vector at N_d DOF at time $t_n = n\Delta t$, where Δt is a prescribed time interval. The input for calculating the model response $\mathbf{q}(n; \boldsymbol{\theta})$ is assumed to be prescribed. For given dynamic test data $\mathcal{D}_N$ consisting of sampled input and output histories, the model prediction error, $\mathbf{e}(n; \boldsymbol{\theta})$, satisfies the relation

$$\mathbf{y}(n) = S_o \mathbf{q}(n; \boldsymbol{\theta}) + S_o \mathbf{e}(n; \boldsymbol{\theta}) \qquad (1)$$

where $\mathbf{y}(n) \in \mathcal{R}^{N_o}, n = 1, ..., N$, are the sampled output histories at N_o observed DOF of the structural model, N is

the number of sampled data, and S_o is a matrix that selects only those degrees of freedom where measurements are made. The prediction error, $\mathbf{e}(n; \boldsymbol{\theta})$, which accounts for modeling errors and measurement noise, is quantified by choosing a class of probability models $\mathcal{P}$, parameterized by a parameter set $\boldsymbol{\sigma}$.

The class of probability models $\mathcal{M}_P$ which is defined by the selection of the classes $\mathcal{M}$ and $\mathcal{P}$, is thus parameterized by $[\boldsymbol{\theta}, \boldsymbol{\sigma}]$. Using Bayes' theorem, the initial ("prior") probability density function (PDF), $p(\boldsymbol{\theta}, \boldsymbol{\sigma} | \mathcal{M}) = \pi(\boldsymbol{\theta}, \boldsymbol{\sigma})$, prescribed as a model for the relative plausibilities of each of the models in $\mathcal{M}_P$ specified by the parameters $[\boldsymbol{\theta}, \boldsymbol{\sigma}]$, is converted to an updated ("posterior") PDF, $p(\boldsymbol{\theta}, \boldsymbol{\sigma} | \mathcal{M}, \mathcal{D}_N)$, which gives the relative plausibilities of the models based on the inclusion of the measured data, $\mathcal{D}_N$, as

$$p(\boldsymbol{\theta}, \boldsymbol{\sigma} | \mathcal{M}, \mathcal{D}_N) = kp(\mathcal{D}_N | \boldsymbol{\theta}, \boldsymbol{\sigma}, \mathcal{M})\pi(\boldsymbol{\theta}, \boldsymbol{\sigma}). \qquad (2)$$

In this updating procedure, the PDF for the system data, $p(\mathcal{D}_N | \boldsymbol{\theta}, \boldsymbol{\sigma}, \mathcal{M})$, depends on the probability model chosen for the prediction error $\mathbf{e}(n; \boldsymbol{\theta})$ at time $t_n = n\Delta t$. In this work, the probability model chosen for the prediction error corresponds to discrete Gaussian white noise where each component of $\mathbf{e}(n; \boldsymbol{\theta})$ is independent with zero mean and a variance of σ^2 which is also updated along with the structural model parameters [17].

For a large number N of available data, it is found that the updated marginal PDF $p(\boldsymbol{\theta} | \mathcal{M}, \mathcal{D}_N)$ of the structural model parameters $\boldsymbol{\theta}$ is given by $p(\boldsymbol{\theta} | \mathcal{M}, \mathcal{D}_N) = cJ(\boldsymbol{\theta})^{-(N_o N - 1)/2}$ and it is concentrated in the neighborhood of a manifold $\mathcal{S}$ in the parameter space. Here, $J(\boldsymbol{\theta})$ is a positive measure-of-fit function between the measured response and the model response at the measured DOFs, defined by

$$J(\boldsymbol{\theta}) = \frac{1}{N_o N} \sum_{n=1}^{N} \|\mathbf{y}(n) - S_o \mathbf{q}(n; \boldsymbol{\theta})\|^2. \qquad (3)$$

For a sufficiently small number of model parameters for updating, the dimension m_s of this manifold $\mathcal{S}$ is zero, that is, the updated PDF is concentrated in the close neighborhood of isolated points in the parameter space. These points are referred to as optimal parameter values, and they correspond to the structural model parameter values which globally minimize $J(\boldsymbol{\theta})$ [17]. They give the most probable parameter values based on the data $\mathcal{D}_N$ alone. Even in the case of linear dynamic models, $J(\boldsymbol{\theta})$ is a non-linear non-convex function of the parameters $\boldsymbol{\theta}$ and, therefore, it may possess multiple global minima [16,28,30] designated by $\hat{\boldsymbol{\theta}}_k$, $k = 1, ..., K$. Thus, when the dimension of $\mathcal{S}$ is zero, there may be a unique optimal parameter (global identifiability; $K = 1$), or a discrete set of optimal parameters (local identifiability; $K > 1$). Under the assumption of a bounded parameter domain, the number of optimal parameters is finite in identifiable cases. The optimal parameters $\hat{\boldsymbol{\theta}}_k$, $k = 1, ..., K$, satisfy $J(\hat{\boldsymbol{\theta}}_1) = \cdots = J(\hat{\boldsymbol{\theta}}_K) = \hat{\sigma}^2$, where $\hat{\sigma}^2$ is the optimal value of the variance of the prediction error. These optimal parameter values therefore

correspond to structural models that have the same response at the measured DOFs to within the accuracy specified by $\hat{\sigma}$.

Algorithms for resolving the problem of finding all optimal parameters in identifiable cases have been presented [16,28,31]. In these cases, the PDF decays rapidly in all directions around each optimal point and the updated PDF can be asymptotically approximated by a weighted sum of Gaussian distributions, centered at the optimal parameters [17]. It is convenient in approximate calculations to further simplify the updated PDF as a weighted sum of Dirac delta functions, instead of Gaussian distributions, centered at the optimal points, that is,

$$p(\boldsymbol{\theta}|\mathcal{M}, \mathcal{D}_n) \approx \sum_{k=1}^{K} w_k \delta(\boldsymbol{\theta} - \hat{\boldsymbol{\theta}}_k) \qquad (4)$$

where each weighting coefficient w_k in this sum reflects the relative volume of the updated PDF contained in the neighborhood of significant probabilities of the corresponding optimal point, $\hat{\boldsymbol{\theta}}_k$. It can be shown that the coefficient w_k is given by [17]

$$w_k = c_1 |A(\hat{\boldsymbol{\theta}}_k)|^{-1/2} \pi(\hat{\boldsymbol{\theta}}_k, \hat{\sigma}) \qquad (5)$$

where the matrix $A(\hat{\boldsymbol{\theta}}_k)$ is the Hessian of the function $(N_\mathrm{o}N/2) \ln J(\boldsymbol{\theta})$ evaluated at $\hat{\boldsymbol{\theta}}_k$, and c_1 is a normalizing coefficient such that $\sum_{k=1}^{K} w_k = 1$. The approximation (4) leads to the correct asymptotic approximations for large sample sizes N for the integrals giving the predictive PDF of the response and the response reliability but the same results can be rigorously derived without using Eq. (4) [17].

In other cases, the number of optimal solutions minimizing $J(\boldsymbol{\theta})$ in Eq. (3) may be either infinite, forming a manifold $\mathcal{S}$ of dimension m_s larger than zero (strictly unidentifiable case), or it may be finite but the decay of the PDF in the neighborhood of the various optimal points may not be rapid enough in all directions ("almost" unidentifiable case). In the latter case, the neighborhoods of significant probabilities corresponding to different optimal points may either overlap, or they may extend over larger regions so that the earlier Gaussian approximation derived for identifiable cases is inaccurate. In this "almost" unidentifiable case, the manifold $\mathcal{S}$, in the close neighborhood of which all points with significant probabilities are contained, is of dimension larger than zero, extending along the directions of the parameter space where the PDF decays slowly. In addition to containing all optimal points, the manifold $\mathcal{S}$ in this case may contain many other points $\boldsymbol{\theta}_s \in \mathcal{S}$ which are "almost" optimal in the sense that their corresponding value of the measure-of-fit function $J(\boldsymbol{\theta}_s)$ is almost equal to the global minimum. Thus, all points along the manifold correspond to structural models which are almost output equivalent in the sense that they give essentially the same response at the measured DOFs to within the accuracy specified by the optimal prediction variance $\hat{\sigma}^2(\boldsymbol{\theta}_s) = J(\boldsymbol{\theta}_s)$.

It has been shown that in unidentifiable cases one can proceed with approximations analogous to identifiable cases. More specifically, making use of the fact that the updated PDF $p(\boldsymbol{\theta}|\mathcal{M}, \mathcal{D}_N)$ decays very rapidly in the direction perpendicular to the manifold $\mathcal{S}$, it can again be conveniently approximated as a weighted "sum" of Dirac delta functions centered at the points of the manifold $\mathcal{S}$ as follows [29]:

$$p(\boldsymbol{\theta}|\mathcal{M}, \mathcal{D}_N) \approx \int_{\mathcal{S}} w(\boldsymbol{\theta}_s) \delta(\boldsymbol{\theta} - \boldsymbol{\theta}_s) \, \mathrm{d}\boldsymbol{\theta}_s \qquad (6)$$

where the weight $w(\boldsymbol{\theta}_s)$ accounts for the volume of the PDF in the neighborhood of each point $\boldsymbol{\theta}_s$ in the direction perpendicular to the manifold, and $\mathrm{d}\boldsymbol{\theta}_s$ denotes integration along the manifold. The weighting function $w(\boldsymbol{\theta}_s)$ is specified for all point $\boldsymbol{\theta}_s \in \mathcal{S}$ by:

$$w(\boldsymbol{\theta}_s) = c_2 J(\boldsymbol{\theta}_s)^{-N_\mathrm{o}N/2} |B(\boldsymbol{\theta}_s)|^{-1/2} \pi(\boldsymbol{\theta}_s, \hat{\sigma}(\boldsymbol{\theta}_s)) \qquad (7)$$

where c_2 is a normalizing constant ensuring that the integral of $w(\boldsymbol{\theta}_s)$ over the manifold $\mathcal{S}$ of dimension m_s is equal to unity, $B(\boldsymbol{\theta}_s)$ is a matrix of dimension $m - m_s$ corresponding to the Hessian of the function $(N_\mathrm{o}N/2) \ln J(\boldsymbol{\theta})$ considered in the subspace which is perpendicular to the manifold $\mathcal{S}$ at the point $\boldsymbol{\theta}_s$, and $\hat{\sigma}^2(\boldsymbol{\theta}_s) = J(\boldsymbol{\theta}_s)$.

The manifold can be adequately represented using a set of closely spaced points on $\mathcal{S}$. Efficient adaptive algorithms for calculating a set of such representative points have been developed [29,32]. The representation (6) is adequate for the response PDF or reliability computations, provided that the response or reliability conditional on $\boldsymbol{\theta}$ varies slowly with $\boldsymbol{\theta}$ over the domain of non-negligible values of the PDF $p(\boldsymbol{\theta}|\mathcal{M}, \mathcal{D}_N)$ in the direction perpendicular to the manifold $\mathcal{S}$. For most practical applications, such a representation is accurate since the PDF decays very rapidly in the direction perpendicular to the manifold $\mathcal{S}$ for large sample sizes N. The representation (6) can be viewed as an extension of the representation (4) to the case for which the manifold $\mathcal{S}$ has dimension $m_s > 0$.

Note that the existence of the manifold $\mathcal{S}$ with dimension lower than the dimension of the original space of model parameters $\boldsymbol{\theta}$ signifies that there is a strong correlation of the model parameters only along the specific manifold $\mathcal{S}$ identified using the test data. Such correlation cannot be quantified by prior subjective PDFs which are based on engineering judgement alone. This strong correlation along certain directions in the parameter space is expected to significantly affect the predictions of response and reliability, especially at the DOF which are not measured.

Note also that the above Bayesian framework for model updating enables one to account for all probable models in a rational manner, and thus overcomes many of the difficulties and limitations faced by most deterministic model updating methodologies. The deterministic methods, such as least-squares methods based on the same measure-of-fit as in Eq. (3), can only handle making predictions using one updated model. They are therefore suitable only for model updating cases which are globally identifiable.

3. Robust reliability and its updating during monitoring

In the updating process, we focus on computing the robust failure probability, the complement of the robust reliability. We start with the probability of failure of a structure with known model parameters, $P(\mathcal{F}|\mathbf{\theta}, \mathcal{M})$, also referred to as the conditional probability of failure. It is assumed herein that $P(\mathcal{F}|\mathbf{\theta}, \mathcal{M})$ is available or it can be evaluated using probabilistic structural analysis tools. For example, for a prescribed future stochastic excitation, this can be approximated using available random vibrations theories, such as Rice's theory using the outcrossing rate [33].

To evaluate the robust failure probability of the system when the system model is uncertain, one must evaluate a weighted integral of the conditional failure probabilities over the whole parameter space. The weighting function in the integral is the PDF of the possible models of the system. In the case where no dynamic data is available, the initial PDF $p(\mathbf{\theta}|\mathcal{M})$ of the model parameters is involved, and the theorem of total probability gives:

$$P(\mathcal{F}|\mathcal{M}) = \int_{\Theta} P(\mathcal{F}|\mathbf{\theta}, \mathcal{M}) p(\mathbf{\theta}|\mathcal{M}) \, d\mathbf{\theta}, \tag{8}$$

where $p(\mathbf{\theta}|\mathcal{M})$ is usually chosen to be of a convenient mathematical form which is roughly consistent with the engineer's judgment regarding the relative plausibilities of each model given by the parameters $\mathbf{\theta}$, and Θ is a subregion of $\mathcal{R}^m$. This integral is difficult to evaluate, unless only a small number of model parameters $\mathbf{\theta}$ are involved so that numerical integration can be performed. Otherwise, more computationally efficient approximations must be used, such as importance sampling methods [3,5,34].

An asymptotic result that has proved effective for efficient approximate calculation of reliability integrals may also be used [5]. The significance of this asymptotic result is that it involves a direct and simple calculation and yet it provides an accuracy comparable to that of second order reliability (SORM) approximations [2]. The implementation of this result involves the maximization of the integrand of the reliability integral (8). It must be noted that more than one "design point", corresponding to multiple local maxima of the integrand, may exist and in this case all (or several) of these points may need to be included in the calculation in order to achieve accurate results [34]. A robust method for finding multiple maxima is presented in Ref. [31].

In the case where dynamic data $\mathcal{D}_N$ are to be used to update the robust failure probability of the system, the updated PDF $p(\mathbf{\theta}|\mathcal{M}, \mathcal{D}_N)$ described earlier replaces the initial PDF in Eq. (8), and the theorem of total probability gives:

$$P(\mathcal{F}|\mathcal{M}, \mathcal{D}_N) = \int_{\Theta} P(\mathcal{F}|\mathbf{\theta}, \mathcal{M}) p(\mathbf{\theta}|\mathcal{M}, \mathcal{D}_N) \, d\mathbf{\theta}. \tag{9}$$

This integral is also difficult to evaluate, unless only a small number of model parameters $\mathbf{\theta}$ are involved. In fact, it is even more difficult to evaluate numerically than the integral (8) because for large amounts of data (large N), $p(\mathbf{\theta}|\mathcal{M}, \mathcal{D}_N)$ is negligible except on the low-dimensional manifold $\mathcal{S}$ in the parameter space Θ which was described in an earlier section. Therefore, an efficient asymptotic approximation for large N is used.

One must distinguish between identifiable and unidentifiable cases. In the identifiable case, the integral for the robust failure probability may be decomposed into a finite sum of integrals over K disjoint subregions of the parameter space, where each subregion contains only one optimal point, $\hat{\mathbf{\theta}}_k$. In each subregion, the aforementioned asymptotic result must be employed. Utilizing the representation (4) for $p(\mathbf{\theta}|\mathcal{M}, \mathcal{D}_N)$, and assuming a large number N of data is available, the robust failure probability of the structure given in Eq. (9) can be well approximated as a weighted sum of the conditional probabilities of failure corresponding to each optimal value of the parameters:

$$P(\mathcal{F}|\mathcal{M}, \mathcal{D}_N) \approx \sum_{k=1}^{K} w_k P(\mathcal{F}|\hat{\mathbf{\theta}}_k, \mathcal{M}) \tag{10}$$

In an unidentifiable case and for a large number N of data, the region of the parameter space contributing to the probability of failure integral is concentrated in a close neighborhood of the manifold $\mathcal{S}$, as discussed in the previous section. In this case, utilizing the representation (6) for the updated probability distribution of the parameters, the integral (9) for the updated failure probability simplifies to the following weighted integral of the conditional probabilities of failure over the manifold $\mathcal{S}$:

$$p(\mathcal{F}|\mathcal{M}, \mathcal{D}_N) \approx \int_{\mathcal{S}} w(\mathbf{\theta}_s) P(\mathcal{F}|\mathbf{\theta}_s, \mathcal{M}) \, d\mathbf{\theta}_s. \tag{11}$$

It can be readily shown that Eq. (11) is asymptotically correct for large number of data. Also, Eq. (10) is a special case of Eq. (11) for which the dimension of the manifold $m_s = 0$. However, the numerical techniques required for calculating the manifold $\mathcal{S}$ in the general case of $m_s > 0$ are substantially different from existing techniques applicable to the case $m_s = 0$ for which the manifold consists of isolated points. Algorithms for the calculation of a low-dimensional manifold $\mathcal{S}$ have been presented [29,32], in which the manifold is represented by a discrete set of points $\mathbf{\theta}_k$, $k = 1, ..., K$, non-uniformly distributed along the manifold $\mathcal{S}$. Using simple numerical integration algorithms to approximate the integral (11), the robust failure probability conditional on the test data is obtained as

$$P(\mathcal{F}|\mathcal{M}, \mathcal{D}_N) \approx \sum_{k=1}^{K} w_k P(\mathcal{F}|\mathbf{\theta}_k, \mathcal{M}). \tag{12}$$

Explicit expressions for the weights w_k are available [29] in the form $w_k = I(\mathbf{\theta}_k) \, w(\mathbf{\theta}_k)$, where $w(\mathbf{\theta}_k)$ is given by Eq. (7) and $I(\mathbf{\theta}_k)$ accounts for the non-uniform distribution of the generated points $\mathbf{\theta}_k$, $k = 1, ..., K$, on the manifold $\mathcal{S}$, as well as accounting for the type of numerical integration formula

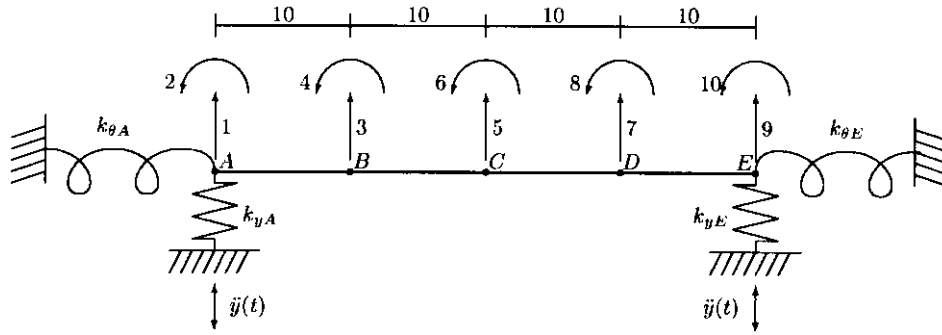Fig. 1. Bridge model.

used. Thus, once the points $\boldsymbol{\theta}_k$, $k = 1, ..., K$, and the corresponding weights w_k are available, the computation of the robust failure probability $P(\mathscr{F}|\mathscr{M}, \mathscr{D}_N)$ is approximated by a weighted sum of the conditional failure probabilities $P(\mathscr{F}|\boldsymbol{\theta}_k, \mathscr{M})$ evaluated at the discrete points $\boldsymbol{\theta}_k$, $k = 1, ..., K$, on the manifold $\mathscr{S}$.

4. Applications

4.1. Bridge on elastic foundation

Consider a single-span bridge and assume that the two-dimensional 10-DOF linear finite element model shown in Fig. 1 simulates its actual behavior. Specifically, the rotational and translational springs at the abutments represent stiffnesses corresponding to soil-structure interaction. The values of the system parameters are: $k_{yA} = 1.1k_y$, $k_{yE} = 0.9k_y$, $k_{\theta A} = 1.2k_\theta$ and $k_{\theta E} = 0.85k_\theta$, where $k_y = 10^7$ N/m and $k_\theta = 10^5$ N m. Also, the bending rigidity of the deck elements AB, BC, CD and DE are $0.95EI$, $1.05EI$, $0.9EI$ and $0.95EI$, respectively, where $EI = 10^9$ N m^2. The lumped masses are equal to $m_A = m_E = 8 \times 10^3$ kg, and $m_B = m_C = m_D = 16 \times 10^3$ kg. The damping is 1% of critical damping in each mode of vibration. In what follows, this model is assumed to be representative of the actual behavior of the bridge structure and is referred to as the actual structure.

In order to simulate modeling errors that are always present in the modeling of actual structures, we define a class of models $\mathscr{M}$ where the stiffness matrix of the model is parameterized by introducing the four non-dimensional parameters: θ_1, θ_2, θ_3 and θ_4, where θ_1 and θ_2 scale the translational spring constants such that $k_{yA} = \theta_1 k_y$, $k_{yE} = \theta_2 k_y$, respectively; θ_3 scales the rotational spring constants such that $k_{\theta A} = k_{\theta E} = \theta_3 k_\theta$; and θ_4 scales the bending rigidity which is assumed to be uniform along the deck with value $\theta_4 EI$. The mass matrix and modal damping for each model in $\mathscr{M}$ is set equal to the exact values for the bridge. Notice that the actual structure does not correspond to any model in the class $\mathscr{M}$. Also, the nominal model of the bridge, which for a real bridge would correspond to a pre-

test finite element model used in the design stages, is taken from the class $\mathscr{M}$ by specifying the values of the model parameters $\boldsymbol{\theta}$.

In this study, the reliability of the structure to future earthquake excitations will be considered. For simplicity, the earthquake excitation is modeled by white noise and the conditional reliability estimates for a particular model of the bridge are based on well-known approximate random vibration results for linear structures. For demonstration purposes, the base motions at the two abutments are assumed to be fully correlated and to have the same spectral density. More realistic descriptions of the ground motion, including spatial correlation [35], could readily be incorporated. However, this is outside the scope of the present example that is concerned primarily with demonstrating the robust reliability updating methodology.

The system is considered to have failed under the earthquake excitation if a response quantity $x(t)$ of the bridge exceeds a threshold level b over a duration T. The objective is to compare the nominal and robust reliability for the bridge at the initial design stage, before any data are collected, with the updated robust reliability at the operational stage during which the test data are collected.

For given model parameters $\boldsymbol{\theta}$, the conditional probability of failure is approximated by [33]

$$P(\mathscr{F}|\boldsymbol{\theta}, \mathscr{M}) = 1 - \exp[-2\nu(\boldsymbol{\theta})T] \tag{13}$$

where $\nu(\boldsymbol{\theta})$ is the rate of outcrossing level b, given by

$$\nu(\boldsymbol{\theta}) = \frac{1}{2\pi} \frac{\sigma_{\dot{x}}(\boldsymbol{\theta})}{\sigma_x(\boldsymbol{\theta})} \exp\left[-\frac{b^2}{2\sigma_x^2(\boldsymbol{\theta})} \right] \tag{14}$$

The quantities $\sigma_x(\boldsymbol{\theta})$ and $\sigma_{\dot{x}}(\boldsymbol{\theta})$ are the standard deviations of the response $x(t)$ and its derivative $\dot{x}(t)$, respectively. These standard deviations of the response are readily obtained for a linear system subjected to white excitation by using the Liapunov equation for the covariance matrix [33,36]. Specifically, consider the state vector $\mathbf{y}(t)$ consisting of response displacements and velocities at the model degrees of freedom of the bridge system. From linear system analysis, the state vector satisfies the state space equation

$$\dot{\mathbf{y}}(t) = A(\boldsymbol{\theta})\mathbf{y}(t) + \mathbf{b}(t) \tag{15}$$
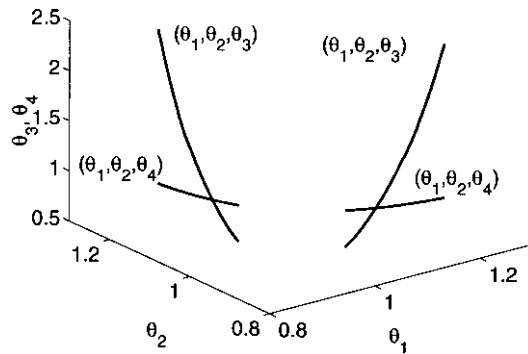
Fig. 2. Manifold of almost optimal models.

where $A(\boldsymbol{\theta})$ is the system matrix depending on the mass, stiffness and damping properties of the bridge, and $\mathbf{b}(t)$ is the white noise excitation vector process. For the stationary case, it is well-known that the covariance matrix $Q_y(\boldsymbol{\theta}) = E[\mathbf{y}\mathbf{y}^{\mathrm{T}}]$ of the state vector satisfies the Liapunov equation

$$A(\boldsymbol{\theta})Q_y(\boldsymbol{\theta}) + Q_y(\boldsymbol{\theta})A^{\mathrm{T}}(\boldsymbol{\theta}) + 2\pi S = 0 \tag{16}$$

where S is the spectral density matrix of the excitation process $\mathbf{b}(t)$. Using the general relationship $\mathbf{z}(t) = C(\boldsymbol{\theta})\mathbf{y}(t)$ between any system response quantities of interest and the state vector, where the matrix $C(\boldsymbol{\theta})$ may depend on the system parameters, the covariance matrix of $\mathbf{z}(t)$ is finally obtained from the relation $Q_z(\boldsymbol{\theta}) = E[\mathbf{z}\mathbf{z}^{\mathrm{T}}] = C(\boldsymbol{\theta})Q_y(\boldsymbol{\theta})C^{\mathrm{T}}(\boldsymbol{\theta})$. The quantities $\sigma_x(\boldsymbol{\theta})$ and $\sigma_{\dot{x}}(\boldsymbol{\theta})$ involved in Eq. (14) are directly obtained by selecting $\mathbf{z} = (x, \dot{x})^{\mathrm{T}}$ in this formulation.

In the design stage, the reliability of the system may be computed using a nominal model or using the set $\mathcal{M}$ of possible models for the bridge. In the first case, the uncertainties in the model are ignored and the bridge is represented by nominal model parameters $\tilde{\boldsymbol{\theta}}$. The nominal failure probability of the system is then simply $P(\mathcal{F}|\tilde{\boldsymbol{\theta}}, \mathcal{M})$. In the second case, uncertainties are included in the modeling and they are quantified by specifying the initial PDF $p(\boldsymbol{\theta}|\mathcal{M})$. The PDF selected to model uncertainty in the model parameters $\boldsymbol{\theta}$ is based on independent and lognormally
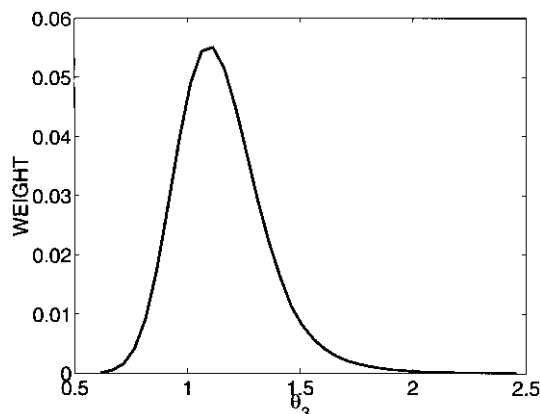

Fig. 3. Weights along manifold.

distributed components θ_i that have their most probable value at the nominal value $\tilde{\theta}_i$ and that have the same coefficient of variation $\gamma_i = 20\%$. The robust failure probability, $P(\mathcal{F}|\mathcal{M})$, of the system is then given by the integral (8). This four-dimensional integral is estimated by two methods, an asymptotic expansion, which is well-suited for approximating the value of this type of probability integral, and an accurate importance sampling method. The details of these methods are described in Ref. [5].

We now suppose that the bridge is built and response data are available to update the model of the bridge and its robust reliability. The model updating is based on measurements of the ground acceleration $\ddot{y}(t)$ at the supports and the absolute acceleration of the translational DOF at the midspan C of the bridge deck, as shown in Fig. 1. Simulated measured data are used in this example. The input ground acceleration history was taken to be the north–south component of the 1940 El Centro earthquake record. The measured response was simulated by first calculating the absolute acceleration response of the structure at the midspan C and then adding 20% rms Gaussian white noise. Twenty seconds of data with sampling interval $\Delta t = 0.02$ s were used, giving a total of $N = 1000$ data points.

It was found that for this example the parameters $\boldsymbol{\theta} = (\theta_1, \theta_2, \theta_3, \theta_4)$ are almost unidentifiable and the set of almost optimal model parameters forms a one-dimensional manifold $\mathcal{S}$ in the four-dimensional parameter space. This manifold was calculated using a new algorithm [29] which represents the manifold $\mathcal{S}$ by a discrete set of points $\boldsymbol{\theta}_k$, $k = 1, \dots, K$, needed in the implementation of Eq. (12). Fig. 2 shows the manifold plotted in the $(\theta_1, \theta_2, \theta_3)$-space and in the $(\theta_1, \theta_2, \theta_4)$-space. Fig. 3 shows an example of the variation with θ_3 of the weights in Eq. (12) corresponding to the points on the manifold. A relatively large uncertainty in the "optimal" values of $\boldsymbol{\theta}$ over the one-dimensional manifold is observed. The updated robust failure probability $P(\mathcal{F}|\mathcal{M}, \mathcal{D}_N)$ for this case is computed using Eq. (12).

The nominal, robust and updated robust failure probabilities, $P(\mathcal{F}|\tilde{\boldsymbol{\theta}}, \mathcal{M})$, $P(\mathcal{F}|\mathcal{M})$ and $P(\mathcal{F}|\mathcal{M}, \mathcal{D}_N)$, respectively, reflect increasing levels of knowledge and sophistication regarding the model uncertainties. These failure probabilities are computed for the following three cases of response $x(t)$: the displacement at the midspan C relative to the average of the left and right abutment displacements (giving a measure of the deck deformation), the restoring moment at the right abutment E, and the displacement of the left abutment A relative to the ground. The results for these three cases are tabulated in Tables 1–3.

In practice, the nominal model is based on idealized modeling assumptions and information available when the structure is designed, so it cannot be expected to reflect the actual behavior of the structure or its behavior after deterioration from severe environmental effects has occurred. To simulate the effects of modeling errors, that is, that the actual structure can be significantly different from the chosen nominal model, the underlying system is kept

Table 1
Failure probability of midspan displacement

$\tilde{\boldsymbol{\theta}}$	Normalized threshold	Nominal	Robust (Asymp.)	Robust (IS)	Updated robust	Actual
1111	6.86	1.00×10^{-4}	9.72×10^{-4}	1.08×10^{-3}	1.78×10^{-4}	1.75×10^{-4}
2111	6.85	1.00×10^{-4}	9.79×10^{-4}	9.96×10^{-4}	1.88×10^{-4}	1.85×10^{-4}
1211	6.85	1.00×10^{-4}	9.79×10^{-4}	9.86×10^{-4}	1.88×10^{-4}	1.85×10^{-4}
1121	6.73	1.00×10^{-4}	8.73×10^{-4}	9.22×10^{-4}	2.75×10^{-4}	2.70×10^{-4}
1112	4.14	1.00×10^{-4}	1.05×10^{-3}	1.06×10^{-3}	1.96×10^{-1}	1.95×10^{-1}
2211	6.83	1.00×10^{-4}	8.49×10^{-4}	1.05×10^{-3}	1.95×10^{-4}	1.92×10^{-4}
1122	4.10	1.00×10^{-4}	9.85×10^{-4}	1.02×10^{-3}	2.10×10^{-1}	2.09×10^{-1}
2222	4.08	1.00×10^{-4}	9.72×10^{-4}	1.05×10^{-3}	2.12×10^{-1}	2.11×10^{-1}

fixed and various choices are made for the nominal model parameters $\tilde{\boldsymbol{\theta}}$. The values of $\tilde{\boldsymbol{\theta}}$ shown in Tables 1–3 are selected to simulate different levels of model error. Most of the choices of the nominal model shown in the first column of these tables lead to a model that is stiffer than the actual system.

For a given assumed nominal values $\tilde{\boldsymbol{\theta}}$, the choice of threshold level b and the strength S_0 of the white noise excitation, representing the capacity and demand in design, is such that the nominal failure probability, $P(\mathscr{F}|\tilde{\boldsymbol{\theta}}, \mathscr{M})$, is equal to 1×10^{-4}. This simulates the situation where engineering designs based on nominal values, $\tilde{\boldsymbol{\theta}}$, of the structural parameters usually correspond to some specified failure probability. It is easily seen from Eqs. (13), (14) and (16) that the failure probabilities depend only on the ratio $b/\sqrt{S_0}$, referred to in this work as the normalized threshold. In Tables 1–3, the values of the ratio $b/\sqrt{S_0}$ which correspond to the nominal failure probability 1×10^{-4} are given in the second column of these tables. The duration T of the response is taken to be ten times the fundamental period of the nominal bridge model. The last column in Tables 1–3 gives the failure probability for the actual bridge model which was used to generate the stimulated "measured" data. Notice that these values change from row to row because the normalized threshold $b/\sqrt{S_0}$ is changed to keep the nominal failure probability (column 2 in the tables) at a constant level.

Comparing the values of the nominal failure probability, $P(\mathscr{F}|\tilde{\boldsymbol{\theta}}, \mathscr{M})$, and the actual failure probability (columns 2 and 6 in the tables), it can be seen that the uncertainties in translational and rotational soil stiffnesses have an important influence on the failure probabilities for the restoring

moment at the right abutment and for the displacement at the left abutment but they have a lesser effect on the displacement at the midspan. This is because the effect of the uncertainties in the abutment stiffnesses gets "smoothed out" to some extent for the midspan response, but not for the response at the abutments where the uncertain soil springs are located. Uncertainties in the bending rigidity of the deck play an important role for all response quantities because the deck is more flexible than assumed in the design.

Columns 3 and 4 in Tables 1–3 give the robust failure probability $P(\mathscr{F}|\mathscr{M})$ using the efficient asymptotic approximation and the accurate importance sampling method, respectively [5]. By comparing columns 3 and 4 in these tables, it can be seen that the results from the asymptotic expansion are sufficiently accurate since they are close to those obtained by the importance sampling method. Comparing the nominal failure probability $P(\mathscr{F}|\tilde{\boldsymbol{\theta}}, \mathscr{M})$ and the robust failure probability $P(\mathscr{F}|\mathscr{M})$, it can be concluded that taking account of modeling uncertainties during design is very important. The robust failure probability is an order of magnitude larger than the nominal failure probability for the mid-span displacement and two orders of magnitude larger for the right-abutment restoring moment and the left-abutment displacement.

The updated robust failure probability $P(\mathscr{F}|\mathscr{M}, \mathscr{D}_N)$ and the actual failure probability are very close (see Table 1) at the measured DOF at the midspan of the bridge which reflects the fact that predictions at measured DOFs are expected to be good for all models $\boldsymbol{\theta}_k$, $k = 1, ..., K$ along the manifold $\mathscr{S}$. However, the updated failure probability at unmeasured DOFs (see Tables 2 and 3) differs from the

Table 2
Failure probability of restoring moment at the right abutment

$\tilde{\boldsymbol{\theta}}$	Normalized threshold	Nominal	Robust (Asymp.)	Robust (IS)	Updated robust	Actual
1111	5.32×10^6	1.00×10^{-4}	1.17×10^{-2}	1.28×10^{-2}	2.33×10^{-2}	1.82×10^{-5}
2111	5.29×10^6	1.00×10^{-4}	1.16×10^{-2}	1.25×10^{-2}	2.49×10^{-2}	2.24×10^{-5}
1211	5.38×10^6	1.00×10^{-4}	1.16×10^{-2}	1.20×10^{-2}	2.14×10^{-2}	1.39×10^{-5}
1121	10.4×10^6	1.00×10^{-4}	1.02×10^{-2}	1.11×10^{-2}	5.87×10^{-6}	0.00
1112	3.23×10^6	1.00×10^{-4}	1.25×10^{-2}	1.38×10^{-2}	4.33×10^{-1}	8.69×10^{-2}
2211	5.33×10^6	1.00×10^{-4}	8.00×10^{-3}	1.19×10^{-2}	2.29×10^{-2}	1.77×10^{-5}
1122	6.36×10^6	1.00×10^{-4}	1.17×10^{-2}	1.20×10^{-2}	3.17×10^{-3}	3.49×10^{-8}
2222	6.33×10^6	1.00×10^{-4}	1.17×10^{-2}	1.30×10^{-2}	3.23×10^{-3}	4.00×10^{-8}

Table 3
Failure probability of displacement at the left abutment

$\tilde{\theta}$	Normalized threshold	Nominal	Robust (Asymp.)	Robust (IS)	Updated robust	Actual
1111	0.431	1.00×10^{-4}	9.74×10^{-3}	1.08×10^{-2}	1.20×10^{-3}	6.43×10^{-7}
2111	0.232	1.00×10^{-4}	2.24×10^{-3}	3.28×10^{-3}	6.48×10^{-1}	2.99×10^{-1}
1211	0.440	1.00×10^{-4}	5.54×10^{-3}	5.69×10^{-3}	7.44×10^{-4}	2.77×10^{-7}
1121	0.432	1.00×10^{-4}	9.55×10^{-3}	9.80×10^{-3}	1.10×10^{-3}	5.60×10^{-7}
1112	0.490	1.00×10^{-4}	4.21×10^{-3}	4.55×10^{-3}	4.01×10^{-5}	1.96×10^{-9}
2211	0.224	1.00×10^{-4}	5.70×10^{-3}	6.79×10^{-3}	7.02×10^{-1}	3.96×10^{-1}
1122	0.491	1.00×10^{-4}	4.20×10^{-3}	4.42×10^{-3}	3.80×10^{-5}	1.79×10^{-9}
2222	0.256	1.00×10^{-4}	9.74×10^{-3}	1.02×10^{-2}	4.27×10^{-1}	7.36×10^{-2}

actual failure probability by several orders of magnitude, depending on the exceedance level b which is different for each row in the tables. This is due to the fact that each of the "output equivalent" models along the manifold $\mathcal{S}$ gives a considerably different response at unmeasured DOFs, while they yield almost the same response at measured DOFs. In all cases, the updated robust failure probability $P(\mathcal{F}|\mathcal{M}, \mathcal{D}_N)$ is higher than the actual failure probability, so it gives a conservative result.

The updated robust failure probability $P(\mathcal{F}|\mathcal{M}, \mathcal{D}_N)$ is conditional on the location and number of sensors, as well as the amount of measured data used. It should be noted that estimates of the updated robust failure probability for the restoring moment at the right abutment and the displacement at the left abutment can be improved by placing additional sensors in the structure or relocating the original sensor. Optimal sensor location methodologies [19,37] can prove to be useful in addressing the issue of obtaining the best reliability estimates from a fixed number of sensors on the structure.

4.2. Bridge with TMD appendage

The bridge described in the previous example is now assumed to be equipped with a TMD attached at its midspan (point C in Fig. 1). For this example, the objective is to perform a robust optimal reliability-based design of the TMD in order to reduce the deformation of the bridge deck during an earthquake. A robust probabilistic control design approach is employed in which the parameters of the TMD are chosen to maximize the target reliability, or, equivalently, to minimize the failure probability [13,14]. Therefore, the reliability of the structure to future earthquake excitations is needed.

The parameters of the TMD to be installed at the midspan of the bridge are the mass, stiffness and damping coefficient which are denoted by m_e, k_e and c_e, respectively. Equivalently, the TMD can be specified by the mass m_e, fixed-based natural frequency $\omega_e = \sqrt{k_e/m_e}$ and the damping ratio $\zeta_e = c_e/2\sqrt{k_e m_e}$. The mass of the TMD is taken to be equal to 5% of the total mass of the bridge. The damping

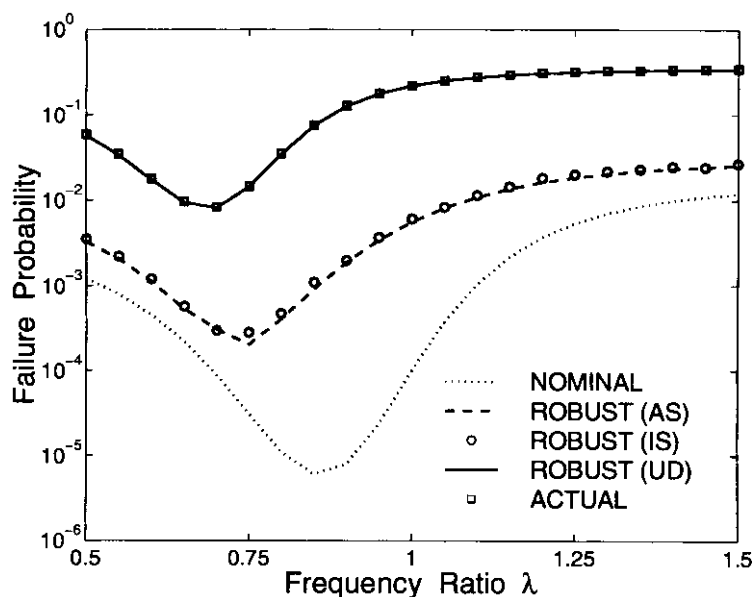Fig. 4. Failure probabilities versus tuning frequency ratio.

ratio, ζ_e, of the TMD is assumed to be 1% of critical damping.

For simplicity and demonstration purposes, the system is considered failed if the displacement response $x(t)$ at the midspan of the bridge exceeds a threshold level b over a duration T. Since a linear model is used, this could be viewed as a serviceability criterion. The conditional probability of failure for given model parameters $\boldsymbol{\theta}$ is given by Eq. (13).

The finite-element model of the bridge obtained during the design phase is assumed to correspond to the nominal model $\tilde{\boldsymbol{\theta}} = (2, 2, 2, 1.5)$. Note that this choice corresponds to an overestimate of the soil spring and bridge deck stiffnesses. This discrepancy between the nominal model and the actual system is purposely considered here to simulate the effects of model error. For example, significant changes in stiffnesses are observed in bridges at large response levels where the equivalent linear model of the bridge is typically much more flexible than an initial finite-element model because of concrete cracking in the main deck and softening of the soil at the abutments.

Given the values of the TMD parameters m_e and ζ_e, the optimal design of the TMD then corresponds to choosing ω_e or, equivalently, to choosing the tuning frequency ratio $\lambda = \omega_e/\tilde{\omega}_1$, where $\tilde{\omega}_1$ is the fundamental frequency of the nominal model of the bridge, in order to minimize the failure probability of the system. The duration T of the response for the reliability calculations is taken to be 10 times the fundamental period of the nominal bridge model. The strength S_0 of the white noise excitation and the threshold level b for the midspan displacement are chosen so that the failure probability for the nominal bridge model is equal to $P(\mathscr{F}|\tilde{\boldsymbol{\theta}}, \mathscr{M}) = 1 \times 10^{-4}$ when the TMD is perfectly tuned to the nominal bridge model (i.e. when $\lambda = 1$). This corresponds to a normalized threshold of $b/\sqrt{S_0} = 5.65$.

Consider the first case where the optimal design of the TMD is performed by minimizing the nominal failure probability, so the uncertainties in the modeling are ignored in the TMD design. The dotted line in Fig. 4 shows the variation of the nominal failure probability $P(\mathscr{F}|\tilde{\boldsymbol{\theta}}, \mathscr{M})$ with the tuning frequency ratio λ. The optimal value of λ for the TMD design is approximately $\lambda_{opt} = 0.87$ corresponding to the minimum of the failure probability $P(\mathscr{F}|\tilde{\boldsymbol{\theta}}, \mathscr{M})$. The line with squares in Fig. 4 shows the failure probability of the actual bridge. The optimal value of λ for the actual bridge model is $\lambda = \omega_e/\tilde{\omega}_1 = 0.68$. If, however, the optimal value of the TMD frequency ω_e is normalized instead by the fundamental frequency ω_1 of the actual bridge, then it corresponds to the optimal ratio $\omega_e/\omega_1 = 0.85$. It is noted that the nominal failure probability is many orders of magnitude less than the failure probability corresponding to the actual bridge system because of the incorrect stiffness values assumed for the nominal model. Furthermore, the optimal design value $\lambda_{opt} = 0.87$ for the TMD based on the nominal bridge model is very sub-optimal for the actual bridge.

The robust failure probability $P(\mathscr{F}|\mathscr{M})$ is also shown in Fig. 4 as a function of the tuning frequency ratio λ, with the dashed line and the circles corresponding to results obtained from the asymptotic method and importance sampling method, respectively [5]. As in the previous example, the model parameters are assumed to be independent and lognormally distributed with most probable values equal to the nominal values $\tilde{\boldsymbol{\theta}}$ and with the same coefficient of variation $\gamma = 20\%$. Two hundred samples were used in the importance sampling method to compute accurate estimates of the failure probabilities. It is obvious from Fig. 4 that the asymptotic method gives results quite close to those computed by the importance sampling method. Also, the robust failure probability $P(\mathscr{F}|\mathscr{M})$ based on modeling uncertainties that are specified solely on engineering judgement is closer to the failure probability for the actual system than $P(\mathscr{F}|\tilde{\boldsymbol{\theta}}, \mathscr{M})$, which is based on the nominal model and does not account for modeling uncertainties. The robust failure probability $P(\mathscr{F}|\mathscr{M})$ achieves a minimum at approximately $\lambda_{opt} = 0.75$. This optimal design value is much closer to the value of $\lambda = 0.68$ that gives the minimum failure probability of the actual bridge. Therefore, use of the robust failure probability which explicitly treats the modeling uncertainties leads to a much better design for the TMD than using the nominal failure probability.

Finally, optimal design of the TMD is performed using the updated robust failure probability $P(\mathscr{F}|\mathscr{M}, \mathscr{D}_N)$ which is computed based on the updated PDF of the model parameters obtained from the system identification procedure described previously. The updated robust failure probability shown in Fig. 4 by the solid line is very close to the failure probability for the actual bridge system, despite the fact that the chosen class of models $\mathscr{M}$ does not include the actual bridge. This closeness illustrates the value of the information gained by the Bayesian system identification method for updating structural models based on response data. Such updating not only helps to better estimate the future response of the structure, but can also lead to prompt corrective actions being taken for upgrading the structural condition or installing control devices after significant changes in structural reliability have been observed during structural health monitoring. For example, the relatively large updated failure probability $P(\mathscr{F}|\mathscr{M}, \mathscr{D}_N)$ indicates that the TMD would not be effective in accomplishing its intended task. Appropriate actions would need to be taken to reduce the response if the initial target failure probability of 1×10^{-4} is to be achieved, perhaps by increasing the mass of the TMD. The optimal value of $\lambda = \omega_e/\tilde{\omega}_1$ corresponding to the minimum of the updated robust failure probability in Fig. 4 is approximately equal to 0.68 or, equivalently, $\omega_e/\omega_1 = 0.85$, and it is clearly very close to the one that minimizes the failure probability of the actual bridge system.

5. Conclusions

The methodology outlined in this work provides a

framework that integrates developments in probabilistic model updating with probabilistic analysis tools in order to update response predictions, in particular structural reliability, based on dynamic data. The proposed methodology could be used during structural health monitoring to update measures of structural safety that could be changing due to deterioration from fatigue or corrosion, or damage induced by severe environmental effects such as earthquakes, water waves and wind loads. Application of the methodology to a beam model of a single-span bridge subjected to earthquake loads, with soil-structure interaction at the abutments and with and without a TMD appendage, shows that the structural reliabilities computed before and after using dynamic data can differ significantly because of the additional information gained about the structure from these data. Therefore, the measured response of a structure, whenever available, should be used to update the lifetime reliability of the structure to give a more accurate picture of its structural safety.

Acknowledgements

References

[1] Breitung K. Asymptotic approximations for multinormal integrals. J Engng Mech, ASCE 1984;110(3):357–66.

[2] Madsen HO, Krenk S, Lind NC. Methods of structural safety. Englewood Cliffs, NJ: Prentice-Hall, 1986.

[3] Schuëller GI, Stix R. A critical appraisal of methods to determine failure probabilities. Struct Safety 1987;4:293–309.

[4] Der Kiureghian A, Lin HZ, Hwang SJ. Second-order reliability approximations. J Engng Mech 1987;113(8):1208–25.

[5] Papadimitriou C, Beck JL, Katafygiotis LS. Asymptotic expansions for reliabilities and moments of uncertain dynamic systems. J Engng Mech, ASCE 1997;123(12):1219–29.

[6] Natke HG, Yao JTP, editors. Structural safety evaluation based on system identification approaches. Proc. of Workshop at Lambrecht/Pfatz, Braunschweig, Germany, 1988. Frieder Vieweg and Son.

[7] Yao JTP, Natke HG. Damage detection and reliability evaluation of existing structures. Struct Safety 1994;15:3–16.

[8] Deodatis G, Asada H, Ito S. Reliability of aircraft structures under nonperiodic inspection—a Bayesian approach. J Engng Fract Mech 1996;53(5):789–805.

[9] Kaspari DC, Spencer BF Jr., Sain MK. Reliability-based optimal control of MDOF structures. Proceedings of Tenth Engineering Mechanics Conference, Boulder, CO, 1995. p. 810–3.

[10] Zhou K, Glover K, Doyle JC. Robust and optimal control. Englewood Cliffs, NJ: Prentice Hall, 1996.

[11] Field Jr. RV, Voulgaris PG, Bergman LA. Probabilistic stability robustness of structural systems. J Engng Mech, ASCE 1996; 111(10):1012–21.

[12] Ben-Haim Y. Robust reliability in the mechanical sciences. Berlin: Springer, 1996.

[13] Papadimitriou C, Katafygiotis LS, Au SK. Effects of structural uncertainties on TMD design: a reliability-based approach. J Struct Control 1997;4(1):65–88.

[14] May BS, Beck JL. Probabilistic control for the active mass driver benchmark structural model. Earthquake Engng Struct Dynamics 1998;27:1331–46.

[15] Beck JL. Statistical system identification of structures. Proc 5th Int Conf on Structural Safety and Reliability, ASCE, II, 1989. p. 1395–402.

[16] Katafygiotis LS. Treatment of model uncertainties in structural dynamics. Technical Report EERL91-01, California Institute of Technology, Pasadena, CA, 1991.

[17] Beck JL, Katafygiotis LS. Updating models and their uncertainties—Bayesian statistical framework. J Engng Mech, ASCE 1998;124(4):455–61.

[18] Beck JL, Vanik MW, Katafygiotis LS. Determination of stiffness changes from modal parameter changes for structural health monitoring. Proc 1st World Conf on Structural Control, Pasadena, CA, 1994.

[19] Papadimitriou C, Beck JL, Au SK. Entropy-based optimal sensor location for structural model updating. J Vibration Control 2000 (in press).

[20] Vanik, MW Beck JL. A Bayesian probabilistic approach to structural health monitoring. Proc 16th IMAC, Santa Barbara, CA, 1998. p. 342–8.

[21] Katafygiotis LS, Lam HF. Probabilistic approach to structural health monitoring using dynamic data. Proc Int Workshop on Structural Health Monitoring, Stanford, CA, 1997.

[22] Sohn H, Law KH. Bayesian probabilistic approach for structural damage detection. Earthquake Engng Struct Dynamics 1997;26: 1259–81.

[23] Sohn H, Law KH. A Bayesian probabilistic damage detection using load-dependent ritz vectors. Proc 16th IMAC, Santa Barbara, CA, 1998. p. 374–80.

[24] Mottershead JE, Friswell MI. Model updating in structural dynamics: a survey. J Sound Vibration 1993;167(2):347–75.

[25] Mottershead JE, Friswell MI. Finite element model updating in structural dynamics. Boston: Kluwer Academic Publishers, 1995.

[26] Doebling S, Farrar C, Prime M, Shevits D. Damage identification and health monitoring of structural and mechanical systems from changes in their vibration characteristics: A literature review. Report no. LA-13070-MS, Los Alamos National Laboratory, Los Alamos, NM, 1996.

[27] Kiremidjian AS, Straser EG, Meng T, Law K, Soon H. Structural damage monitoring for civil structures. Proc. Int. Workshop on Structural Health Monitoring, Stanford, CA, 1997. p. 371–82.

[28] Katafygiotis LS, Beck JL. Updating models and their uncertainties—model identifiability. J Engng Mech, ASCE 1998;124(4):463–7.

[29] Katafygiotis LS, Papadimitriou C, Lam HF. A probabilistic approach to structural model updating. Int J Soil Dynamics Earthquake Engng 1998;17(7–8):495–507.

[30] Udwadia FE. Some uniqueness related to soil and building structural identification. SIAM J Appl Math 1985;45:674–85.

[31] Yang CM, Beck JL. Generalized trajectory methods for finding multiple extrema and roots of functions. J Optim Theory Appl 1998;97(4): 211–27.

[32] Katafygiotis LS, Lam HF. A methodology for treating unidentifiability in model updating. Proc Fourth Int Conf on Stochastic Structural Dynamics, Notre Dame, IN, 1998.

[33] Lin YK. Probabilistic theory of structural dynamics. New York: McGraw Hill, 1967.

[34] Au SK, Papadimitriou C, Beck JL. Treatment of multiple design points in reliability methods. Struct Safety 1999;21:113–33.

[35] Zerva A. Response of multi-span beams to spatially incoherent seismic ground motions. Earthquake Engng Struct Dynamics 1990;19:819–32.

[36] Lutes LD, Sarkani S. Stochastic analysis of structural and mechanical vibrations. Englewood Cliffs, NJ: Prentice-Hall, 1997.

[37] Udwadia FE. Methodology for optimal sensor locations for parameters identification in dynamic systems. J Engng Mech, ASCE 1994;120(2):368–90.